



Phase Structure of QCD matter under extreme conditions and holographic GW

Defu Hou

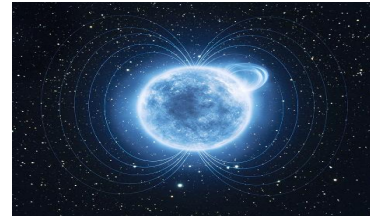
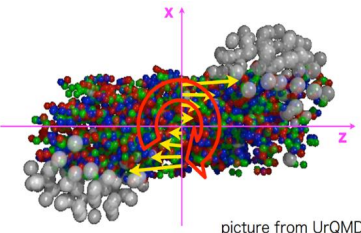
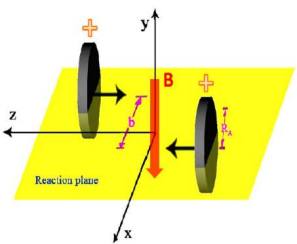
Central China Normal University

Quarks and Compact Stars , Yangzhou University, Sept. 22-26, 2023

Outlines

- **Introduction and motivation**
- **Phase structure under rotation & Magnetic field**
- **Eos Ns structure**
- **GW from 1stOPT**
- **Summary**

Phase structure under new extrem condition

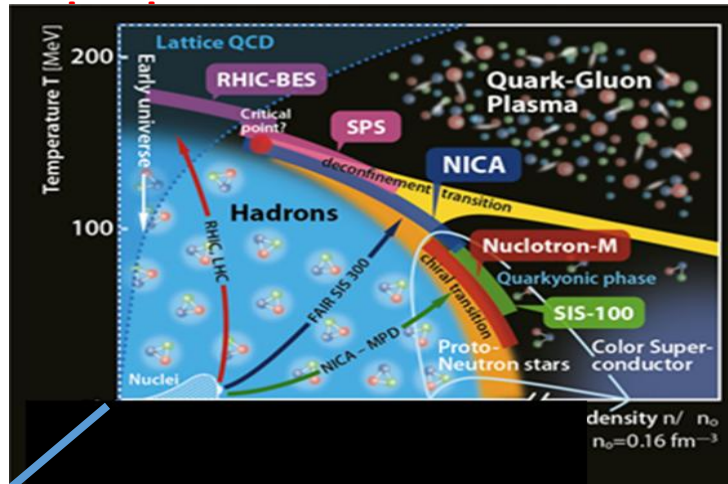


Largest local rotation

What are their effects on the QCD phase

Explore the new dimensions of the QCD phase diagram

B, ω , E, ni...



New theoretical techniques needed!

Lattice QCD

difficulty with Finite baryon density, Real time dynamics Continuum

Phenom. models: (p)NJL、(p)QMC...

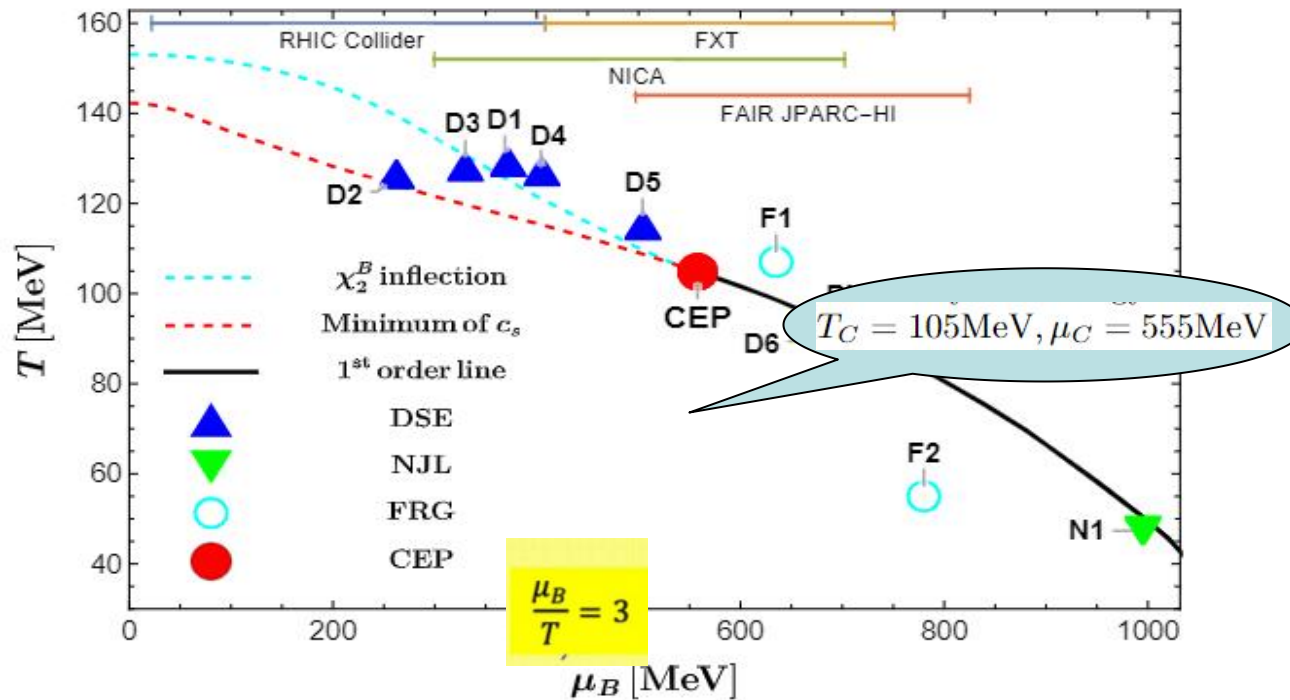
Field Theory: HD(T)L , pQCD , xPT, DSE

Functional Renormalization Group, Sum rules ...

AdS/CFT, AdS/QCD

Predictions of QCD phase diagram

A. Bazavov, etc.Phys. Rev. D 95 (2017) no.5, 054504 [arXiv:1701.04325 [hep-lat]].



(DSE): 2109.09935 [hep-ph], 1607.01675 [hep-ph], 1011.2876 [nucl-th], 1403.3797, 1405.4762, 2002.07500

(NJL, PNJL): arXiv:1801.09215 [hep-ph]], Nucl. Phys. A 504 (1989), 668-684

(FRG); Fu, Pawloski, Rennecke, PRD101(2020); 1909.02991

Zhang, Hou, Kojo, Qin, PRD96 (2017) 1709.05654 [hep-ph]].

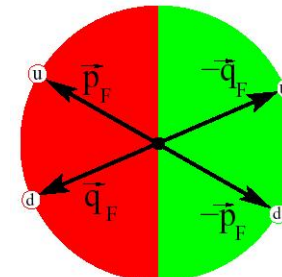
Phase structures in CSC

- BSC-like pairing

J=0: 2SC: u_r, d_r, u_g, d_g

CFL: all flavor and color

M. Alford, K. Rajagopal and F. Wilczek, NPB 537, 443 (1999)



J=1: CSL

T. Schaefer, PRD 62, 094007 (2000)

A. Schmitt, PRD 71, 054016 (2005)

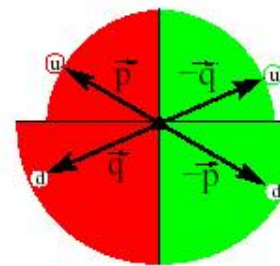
- Non-BCS pairing
gapless CSC
LOFF

Shovkovy and M. Huang, PLB 546, 205 (2003)

M. Alford et al., PRL 92, 222001 (2004)

M. Alford et al., PRD 63, 074016 (2001)

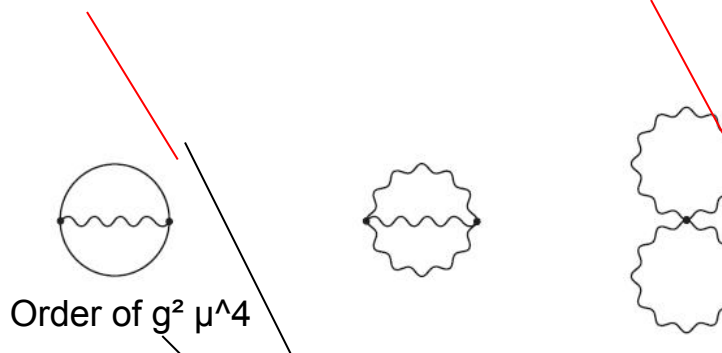
.....



CJT effective action of QCD

$$\Gamma[\bar{D}, \bar{S}] = \frac{1}{2} \{ Tr \ln \bar{D}^{-1} + Tr(D^{-1}\bar{D} - 1) - Tr \ln \bar{S}^{-1} - Tr(S^{-1}\bar{S}) - 2\Gamma_2[\bar{D}, \bar{S}] \}$$

2-loop approximation



Stationary points

$$\left. \frac{\delta \Gamma}{\delta \bar{D}} \right|_{\bar{D}=\bar{D}, \bar{S}=\bar{S}} = 0, \quad \left. \frac{\delta \Gamma}{\delta \bar{S}} \right|_{\bar{D}=\bar{D}, \bar{S}=\bar{S}} = 0$$

$$\bar{D}^{-1} = D^{-1} + \Pi[\bar{S}] \quad \bar{S}^{-1} = S_0^{-1} + \Sigma$$

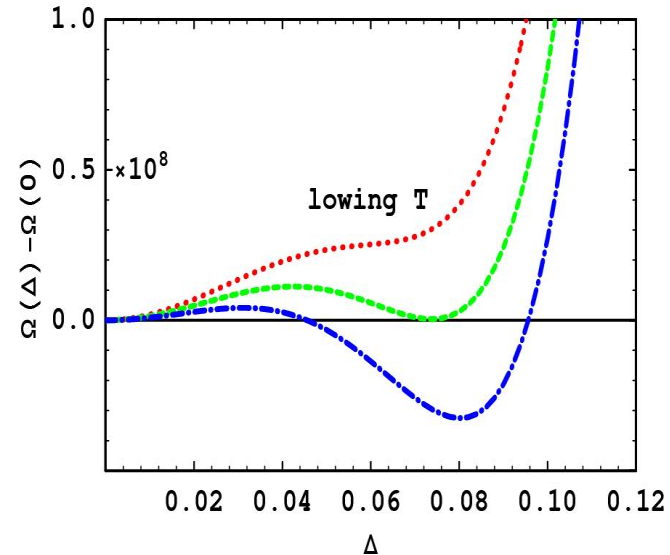
D. Rischke Prog. Part. Nucl. Phys. 52 197 (2004)

$$\Gamma_2[\bar{D}, \bar{S}] = -\frac{1}{2} \text{Tr}\{\bar{D} \Pi[\bar{S}]\}$$

Gauge field fluc. induce 1st order PT of CSC in dense QCD

Ginnakis, Hou, Ren, Rischke, PRL 93 (04) ; PRD73 (06)

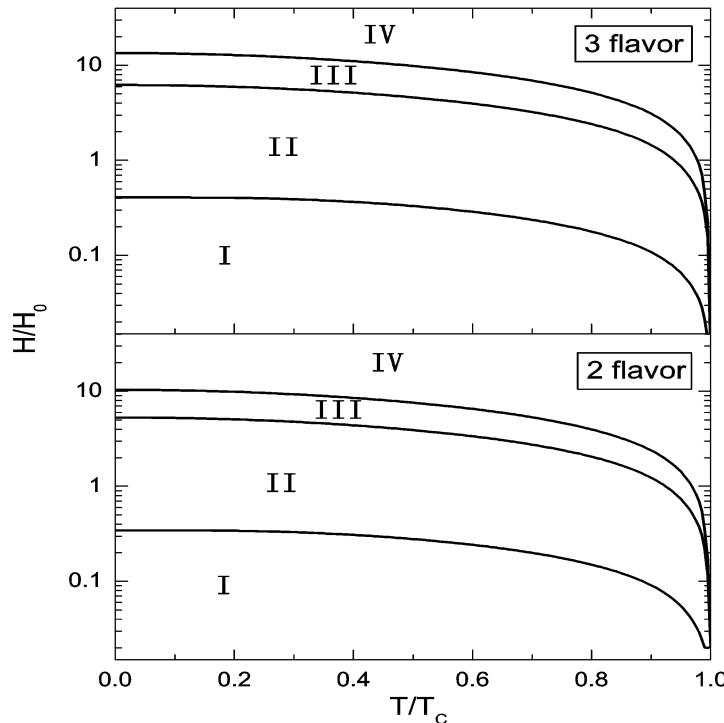
$$\Gamma_{cond} = \frac{1}{4} \text{ (diagram 1)} - \frac{1}{4} \text{ (diagram 2)} - \frac{1}{2} \text{ (diagram 3)} + \frac{1}{2} \text{ (diagram 4)} \\ - \frac{3}{8} \text{ (diagram 5)} - \frac{3}{2} \text{ (diagram 6)} + \frac{1}{4} \text{ (diagram 7)}, \\ \frac{1}{2} \text{ (diagram 8)} + \frac{1}{3} \text{ (diagram 9)} + \frac{1}{4} \text{ (diagram 10)}$$



Introduction of Δ^3 term in free energy by flucs. Inducing 1st order PT in stead of 2nd order PT in MFA

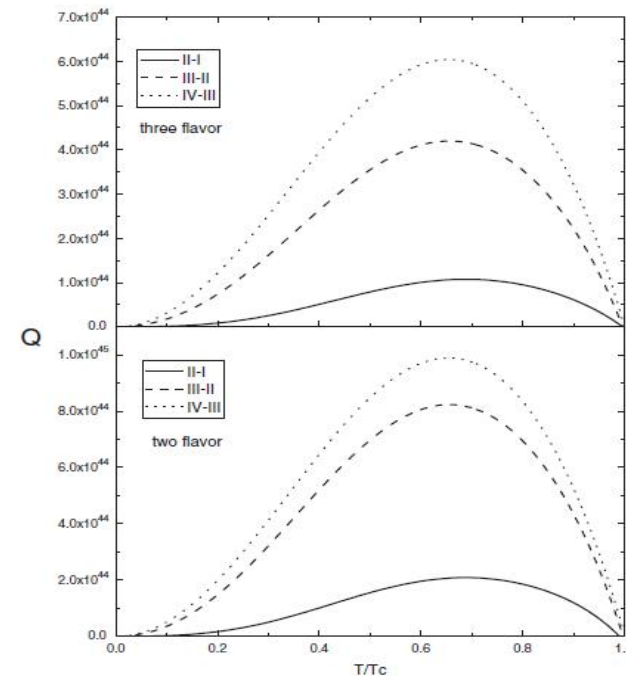
Nonspherical states in dense QCD with B

	I	II	III	IV	$T_C(10^{-1} \text{ MeV})$
Two-flavor	$\text{CSL}_u, \text{CSL}_d$	$(\text{polar})_u, (\text{planar})_d$	$(\text{normal})_u, (\text{polar})_d$	$(\text{normal})_u, (\text{normal})_d$	1.35
Three-flavor	$\text{CSL}_u, \text{CSL}_{d,s}$	$(\text{polar})_u, (\text{planar})_{d,s}$	$(\text{normal})_u, (\text{polar})_{d,s}$	$(\text{normal})_u, (\text{normal})_{d,s}$	0.49



Feng, Hou, Ren,Wu, PRL 105(2010)

$$H_0 = 5.44 \times 10^{14} \text{ G}, 1.97 \times 10^{14} \text{ G}$$



Wu, He, Hou, Ren, PRD84 (2011)

FRGE and phase structure

FRG flow equation

- For continuum field theory
- Non-perturbative
- (known) microscopic laws → complex macroscopic phenomena
- Flow from classical action $S[\phi]$ to effective action $\Gamma[\phi]$
- Scale dependent effective action $\Gamma_k[\phi]$

Wetterich, PLB301, 90 (1993).

Talk in this WS: K. Youngman

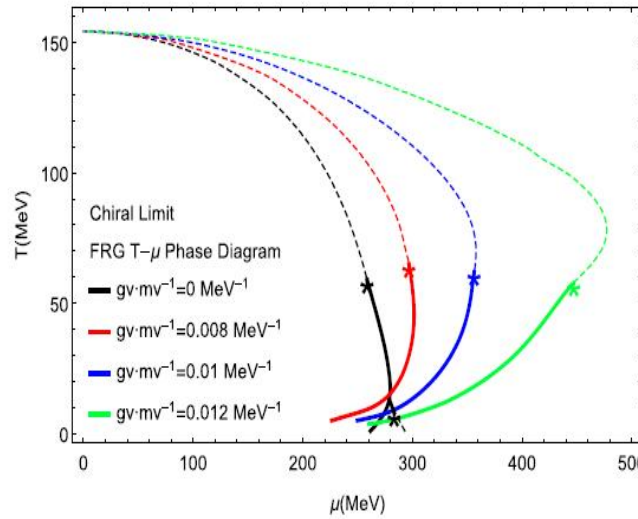
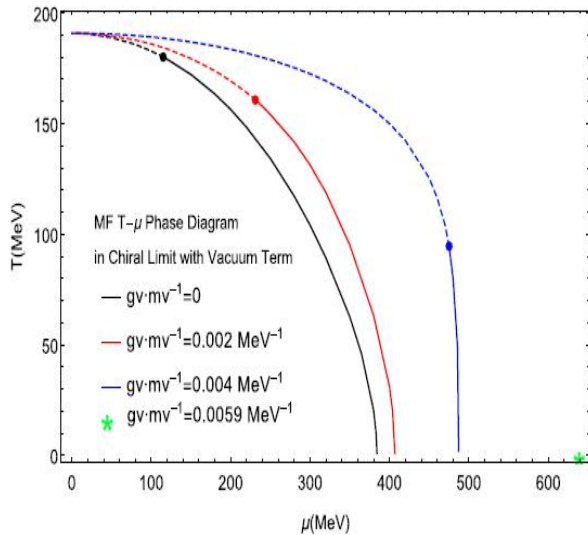
$$\partial_k \Gamma_k = \frac{1}{2} \left(\text{Diagram A} - \text{Diagram B} \right)$$

Diagram A: A circle with a dashed outer boundary and a solid inner boundary. A light blue shaded region is located in the upper-left quadrant of the interior.

Diagram B: A circle with a solid outer boundary and a light red shaded region in the upper-right quadrant of the interior.

FRGE study of phase diagram: Flucts on CEP

Zhang, Hou , Kojo, Qin, PRD96 (2017)



AdS/CFT correspondence

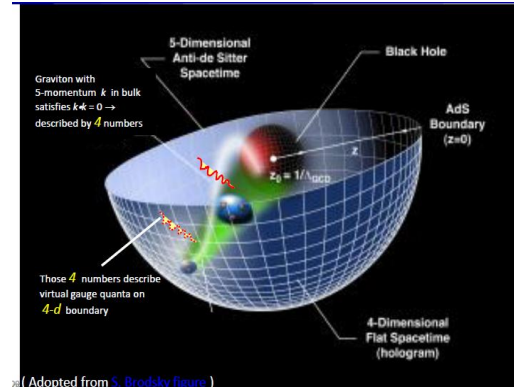
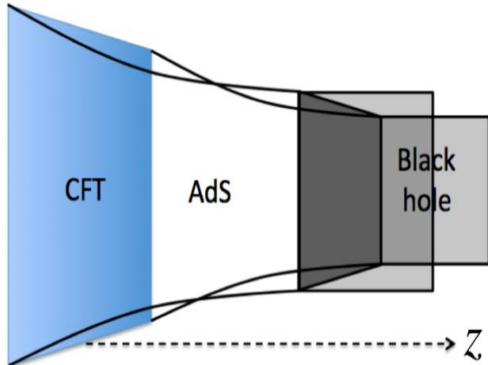
4dim. Large- N_c strongly coupled
 $SU(N_c)$ $N=4$ SYM (finite T).

Maldacena '97



conjecture

Witten '98



Type II B Super String theory on $AdS_5 \text{-} BH \times S^5$

Some complicated Field theory calculations become simple “geometric” problems in higher dimensions

Phase Structure of hQCD with magnetic field

The Einstein-Maxwell-dilaton(EMD) action *:

$$S = -\frac{1}{16\pi G_5} \int d^5x \sqrt{-g} [R - \frac{f_1(\phi)}{4} F_{(1)MN} F^{MN} - \frac{f_2(\phi)}{4} F_{(2)MN} F^{MN} - \frac{1}{2} \partial_M \phi \partial^M \phi - V(\phi)],$$

chemical potential
B field
breaking conformal sym.

The metric:

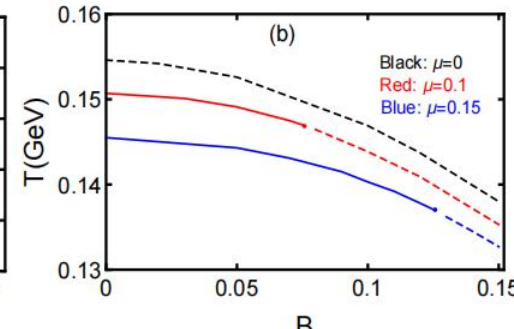
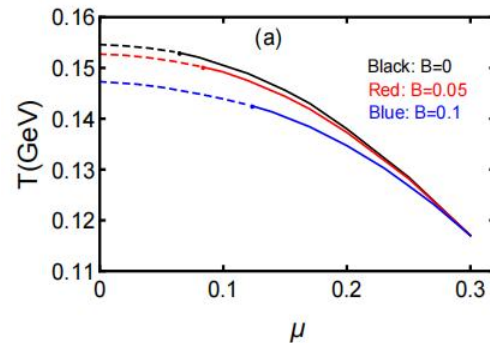
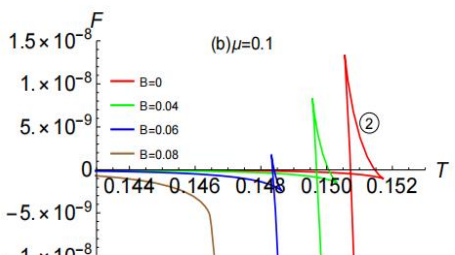
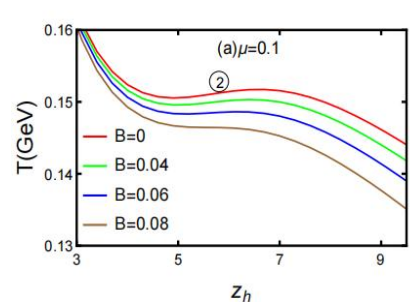
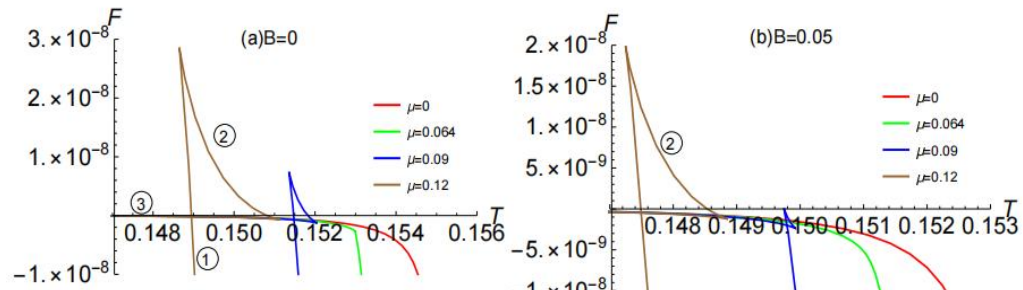
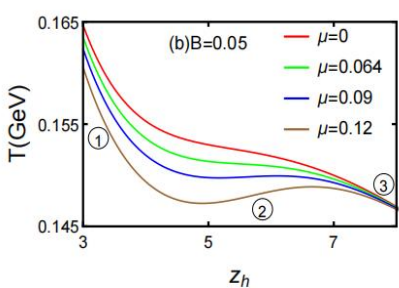
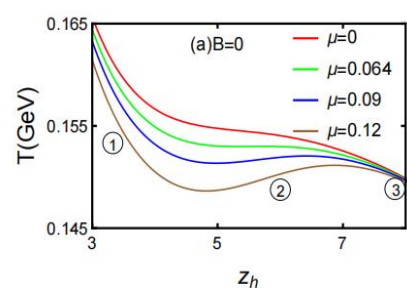
$$ds^2 = \frac{L^2 e^{S(z)}}{z^2} [-g(z)dt^2 + dx_1^2 + e^{B^2 z^2} (dx_2^2 + dx_3^2) + \frac{dz^2}{g(z)}], \quad A_t(z) = \mu [1 - \frac{\int_0^z d\xi \frac{\xi e^{-B^2 \xi^2}}{f_1(\xi) \sqrt{S(\xi)}}}{\int_0^{z_h} d\xi \frac{\xi e^{-B^2 \xi^2}}{f_1(\xi) \sqrt{S(\xi)}}}] = \tilde{\mu} \int_z^{z_h} d\xi \frac{\xi e^{-B^2 \xi^2}}{f_1(\xi) \sqrt{S(\xi)}},$$

Dilaton field :

$$\phi(z) = \int dz \sqrt{-\frac{2}{z} (3zA''(z) - 3zA'(z)^2 + 6A'(z) + 2B^4 z^3 + 2B^2 z)} + K_5.$$

*Hardik Bohra a, David Dудal et al, Anisotropic string tensions and IMC from a dynamical AdS/QCD model. PLB 801 (2020) 135184.

Phase Structure with magnetic field



- 1) μ makes cross over to 1st order PT; B vice versa;
- 2) inverse Magnetic catalysis.

Zhou-Run Zhu, De-fu Hou, (arXiv:2305.12375).

Zhou-Run Zhu, Jun-Xia Chen, Xian-Ming Liu, De-fu Hou, Eur.Phys.J.C 82 (2022) 6,560.

QCD Phase Diagram with rotation

➤ Holographic model:

[1].*Phys.Rev.D* 106 (2022) 12, L121902 • e-Print: 2201.02004

➤ The action:

$$S_M = \frac{1}{2\kappa_N^2} \int d^5x \sqrt{-g} [\mathcal{R} - \frac{1}{2} \nabla_\mu \phi \nabla^\mu \phi - \frac{Z(\phi)}{4} F_{\mu\nu} F^{\mu\nu} - V(\phi)],$$

where the potential and kinetic functions read

$$V(\phi) = -12 \cosh [c_1 \phi] + \left(6c_1^2 - \frac{3}{2}\right) \phi^2 + c_2 \phi^6,$$

Capturing the behavior of EOS at zero chemical potential.

$$Z(\phi) = \frac{1}{1+c_3} \operatorname{sech}[c_4 \phi^3] + \frac{c_3}{1+c_3} e^{-c_5 \phi}.$$

Capturing the flavor dynamic.

➤ The metric:

$$ds^2 = -e^{-\eta(r)} f(r) dt^2 + \frac{dr^2}{f(r)} + r^2 (dx_1^2 + dx_2^2 + dx_3^2),$$

$$\phi = \phi(r), \quad A_t = A_t(r),$$

➤ The Hawking temperature and entropy density:

$$T = \frac{1}{4\pi} f'(r_h) e^{-\eta(r_h)/2} \quad s = \frac{2\pi}{\kappa_N^2} r_h^3.$$

effective Newton constant

Phase diagram @2+1 flavor

➤ Holographic model *with rotation*:

- To introduce the rotation effect, we split the 3-dimensional space into two parts as $\mathcal{M}_3 = \mathbb{R} \times \Sigma_2$. Then the metric becomes to

$$ds^2 = -f(r)e^{-\eta(r)}dt^2 + \frac{dr^2}{f(r)} + r^2\ell^2d\theta^2 + r^2d\sigma^2 \quad \text{where } d\sigma^2 \text{ denotes the line element of } \Sigma_2.$$

- We assume the system that has an angular velocity ω with a fixed radius ℓ , and consider the following local Lorentz boost

[5].JHEP 07 (2021) 132 • e-Print: 2010.14478 [6].Phys.Rev.D 97 (2018) 2, 024034 • e-Print: 1707.03483
 [7].JHEP 04 (2017) 092 • e-Print: 1702.02416 [8].Gen.Rel.Grav. 42 (2010) 1571-1583 • e-Print: 0911.2831

$$t \rightarrow \frac{1}{\sqrt{1 - \omega^2\ell^2}}(\hat{t} + \omega\ell^2\hat{\theta}), \quad \theta \rightarrow \frac{1}{\sqrt{1 - \omega^2\ell^2}}(\hat{\theta} + \omega\hat{t}).$$

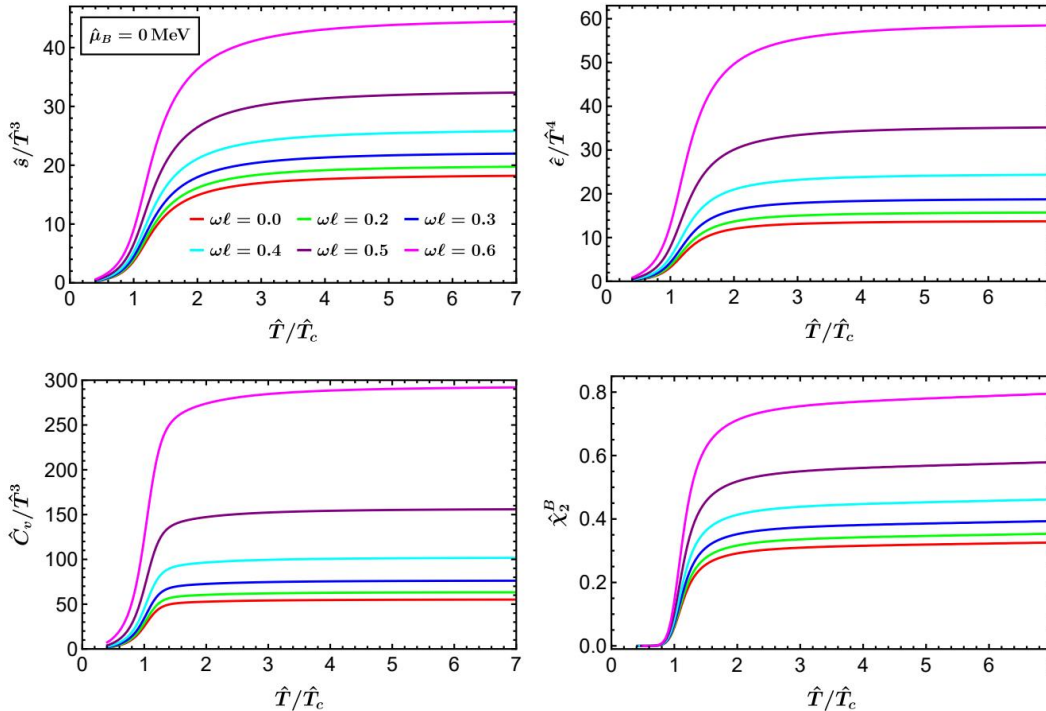
- The corresponding metric can be written as

$$d\hat{s}^2 = g_{\mu\nu}d\hat{x}^\mu d\hat{x}^\nu = -N(r)d\hat{t}^2 + \frac{dr^2}{f(r)} + R(r)(d\hat{\theta} + Q(r)d\hat{t})^2 + r^2d\sigma^2,$$

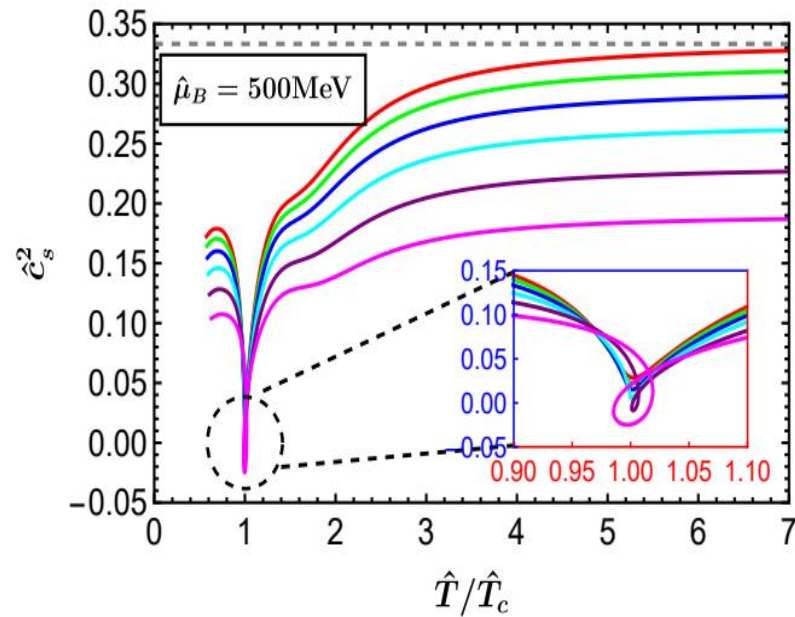
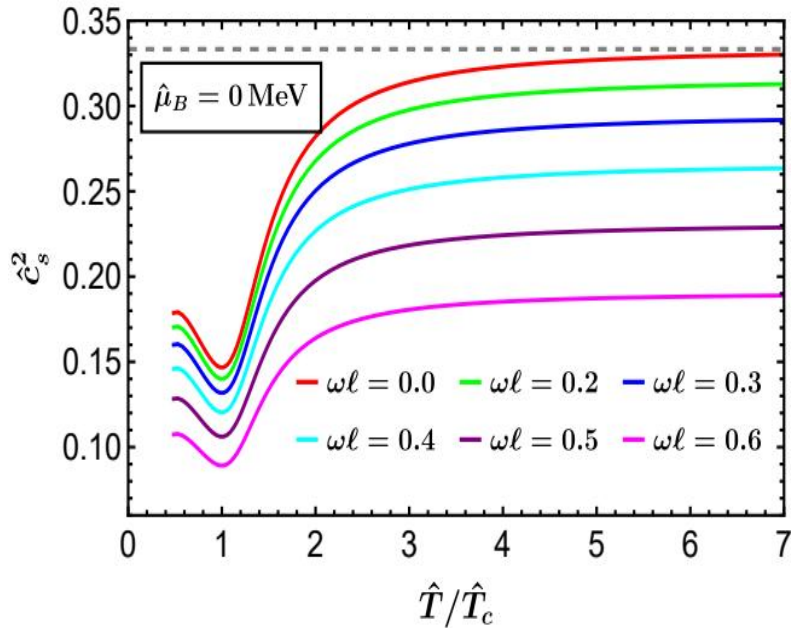
$$\begin{aligned} N(r) &= \frac{r^2 f(r) (1 - \omega^2 \ell^2)}{r^2 e^{\eta(r)} - \omega^2 \ell^2 f(r)}, \\ R(r) &= \frac{r^2 \ell^2 - \omega^2 \ell^4 f(r) e^{-\eta(r)}}{1 - \omega^2 \ell^2}, \\ Q(r) &= \frac{\omega (f(r) - r^2 e^{\eta(r)})}{\omega^2 \ell^2 f(r) - r^2 e^{\eta(r)}}. \end{aligned}$$

Phase diagram @2+1 flavor

➤ Thermodynamics *with rotation*:

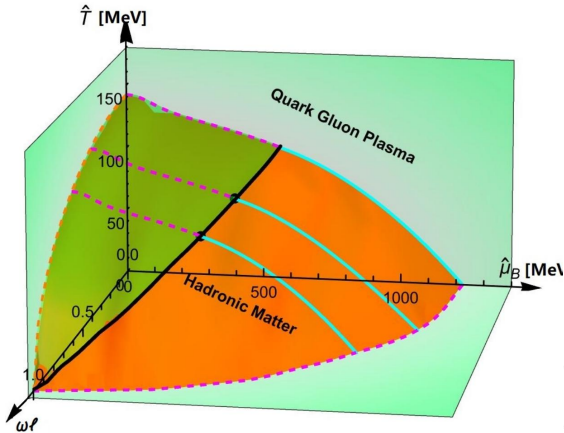


➤ Thermodynamics *with rotation*:



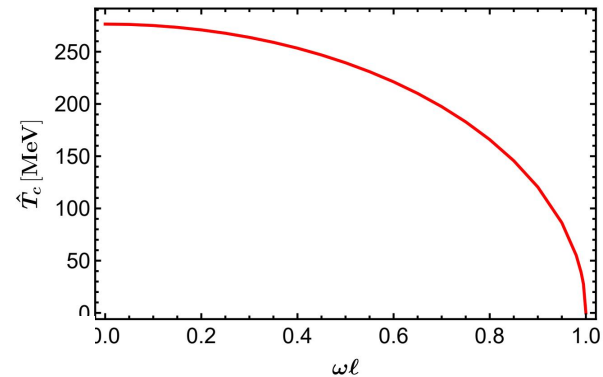
➤ 2+1 flavor:

- ✓ **black solid line:** denoting the location of CEP.
- ✓ At high \hat{T} and small $\hat{\mu}_B$: Being the smooth crossover.
- ✓ At low \hat{T} and large $\hat{\mu}_B$: Being 1st-order transition.
- ✓ $\omega \uparrow$ $\hat{T}_c \downarrow$, $\hat{\mu}_c \downarrow$, $\hat{T}_{cep} \downarrow$, $\hat{\mu}_{cep} \downarrow$.



➤ Pure gluon ($\hat{\mu}_B = 0$):

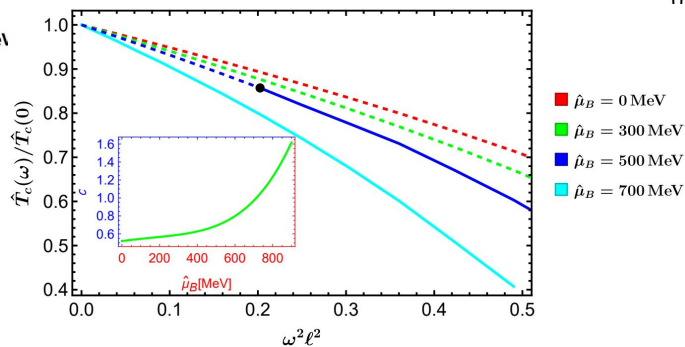
Analytically : $\hat{T}_c(\omega) = T_c \sqrt{1 - \omega^2 \ell^2}$

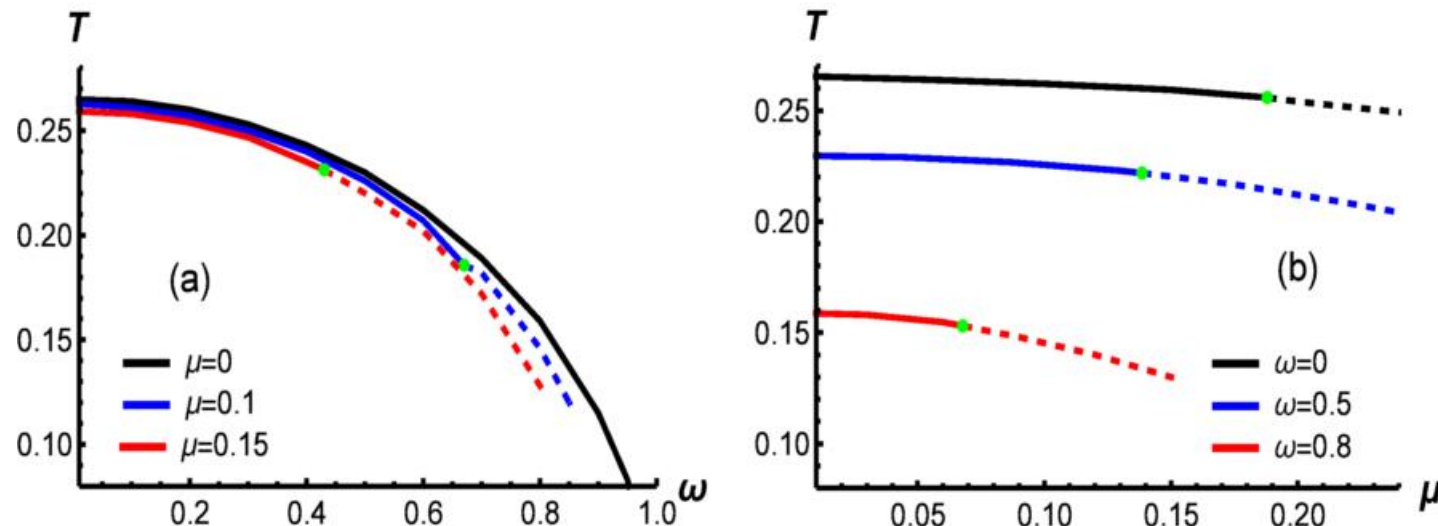


$$\hat{T}_c(\omega) / \hat{T}_c(0) \approx 1 - c \omega^2$$

✓ At finite $\hat{\mu}_B$ and smaller ω .

The value of c depends on $\hat{\mu}_B$.

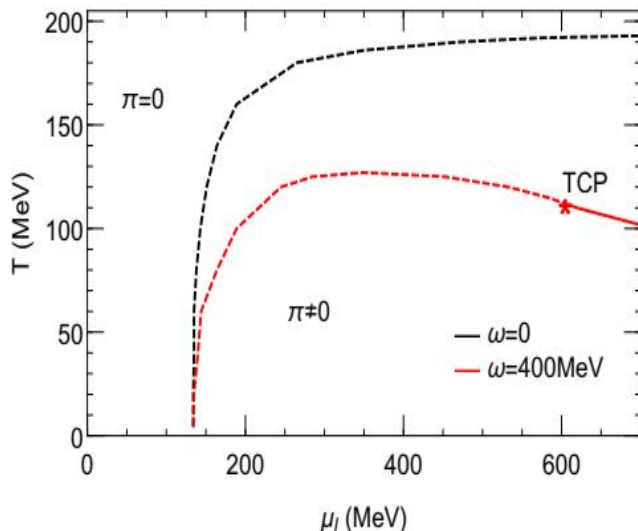




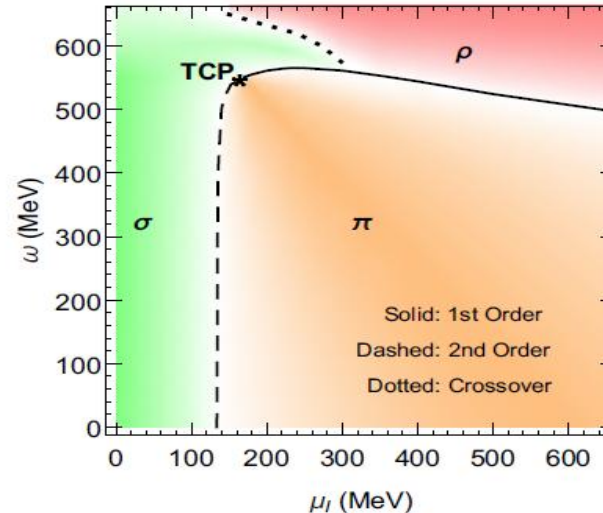
X.Chen, L. Zhang, D.N. Li, D. Hou , M.Huang ,JHEP 07 (2021) 132

New mesonic superfluid phase diagram

H. Zhang, DF Hou, JF Liao, NPA 1005 (2021) 121762



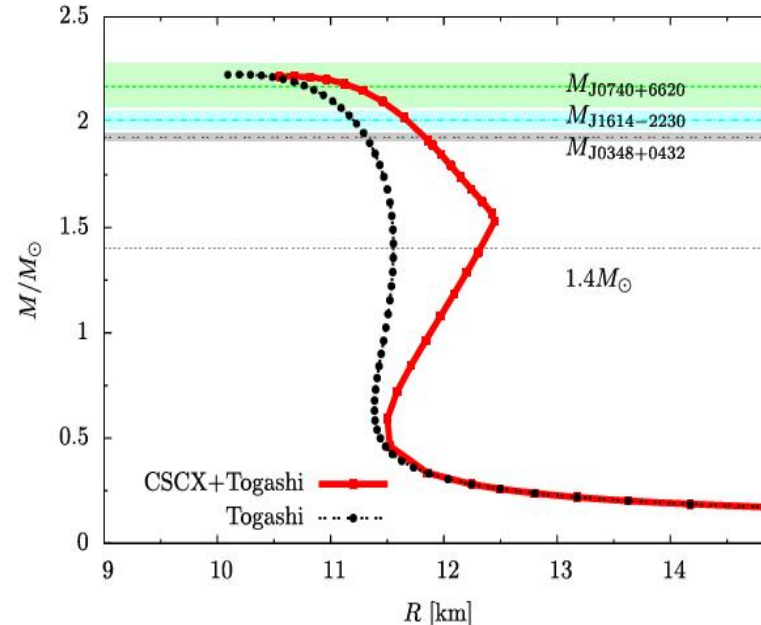
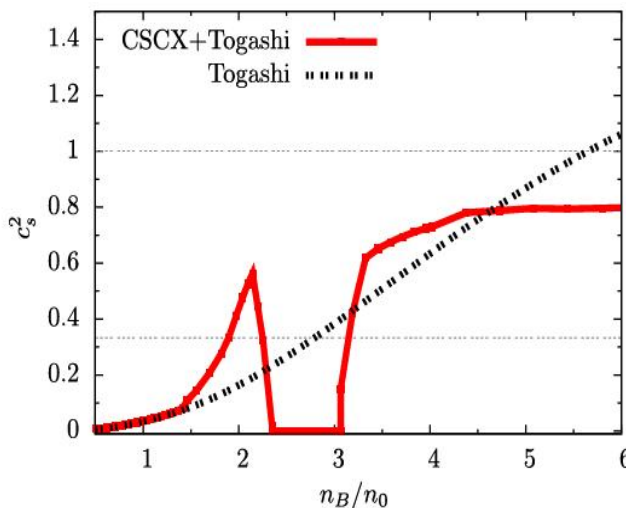
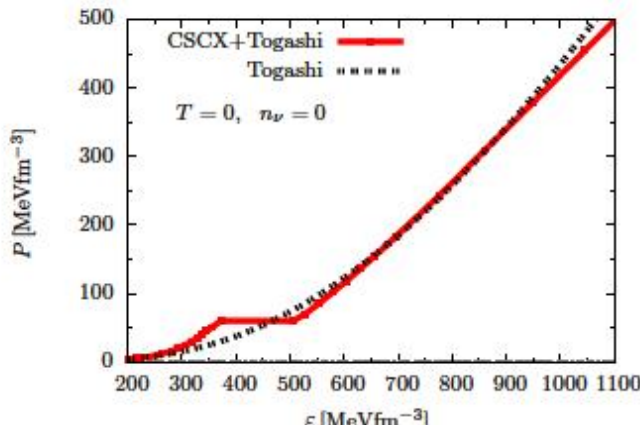
Rotation enhances spin 1 condensate , suppresses spin-zero condensates



H. Zhang, DF Hou, JF Liao. CPC44, No. 11 (2020) 1

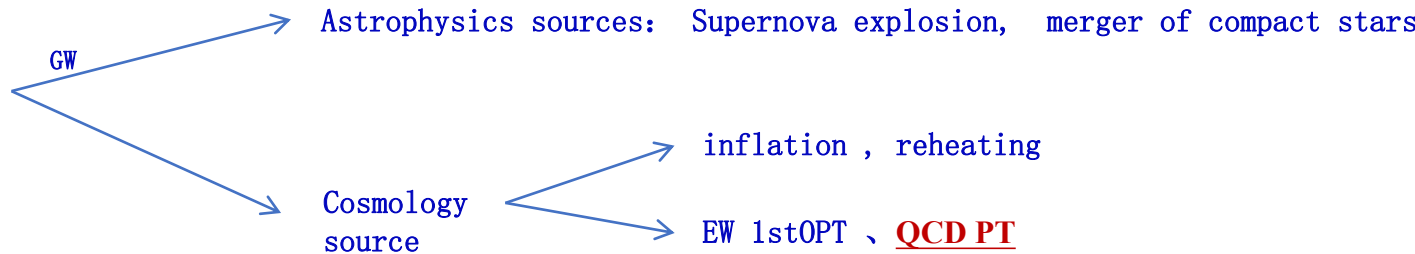
Rotational suppression of Pion superfluid

EOS of QCD Matter and Structure of NSs



T. Kojo , Hou, J. Okafor, H. Togashi, PRD 104 (2021) 063036

GW from Holographic QCD Phase Transition

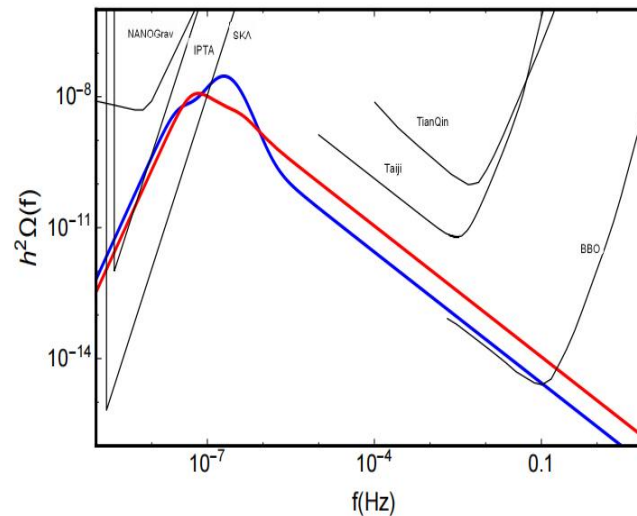
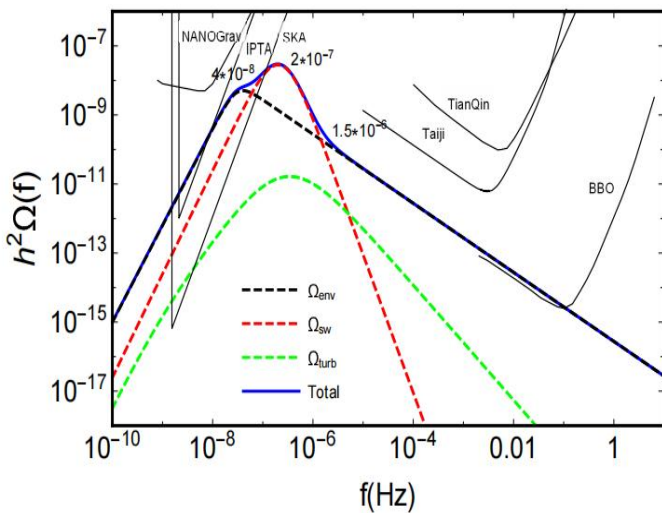


$$h^2\Omega_{env}(f) \quad \text{bubble collision}$$

$$h^2\Omega(f) = h^2\Omega_{env}(f) + h^2\Omega_{sw}(f) + h^2\Omega_{turb}(f)^* \quad h^2\Omega_{sw}(f) \quad \text{Sound wave}$$

$$h^2\Omega_{turb}(f) \quad \text{Turbulent}$$

C. Caprini, M. Hindmarsh, S. Huber, T. Konstandin, J. Kozaczuk, G. Nardini, J. M. No, A. Petiteau, P. Schwaller and G. Servant, et al. JCAP 04 (2016), 001



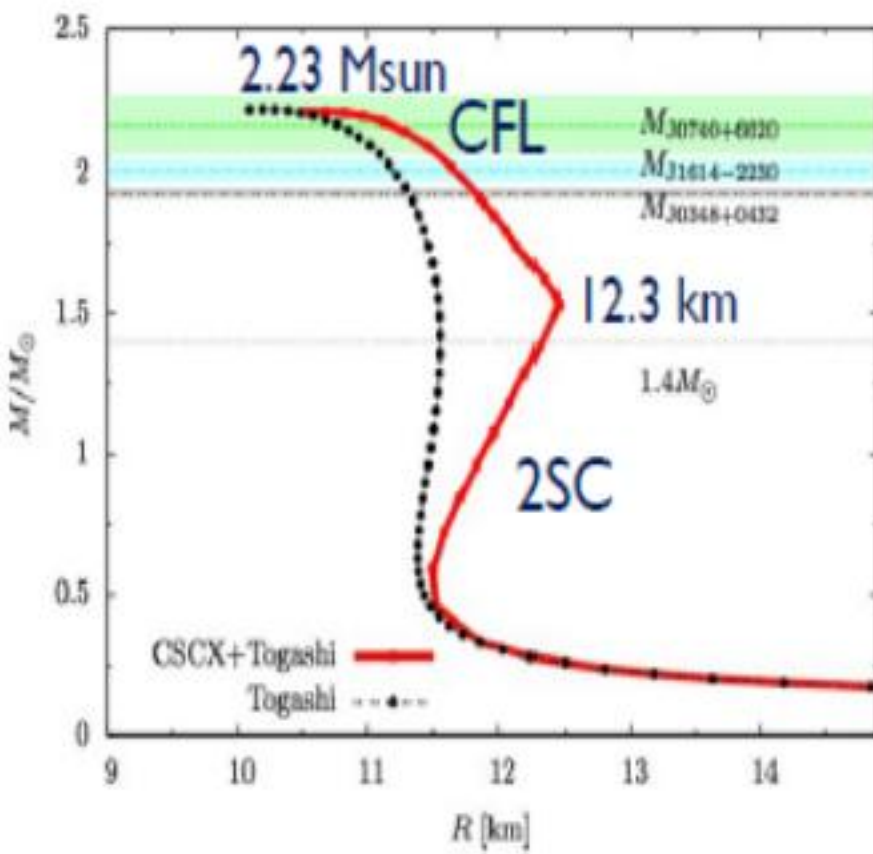
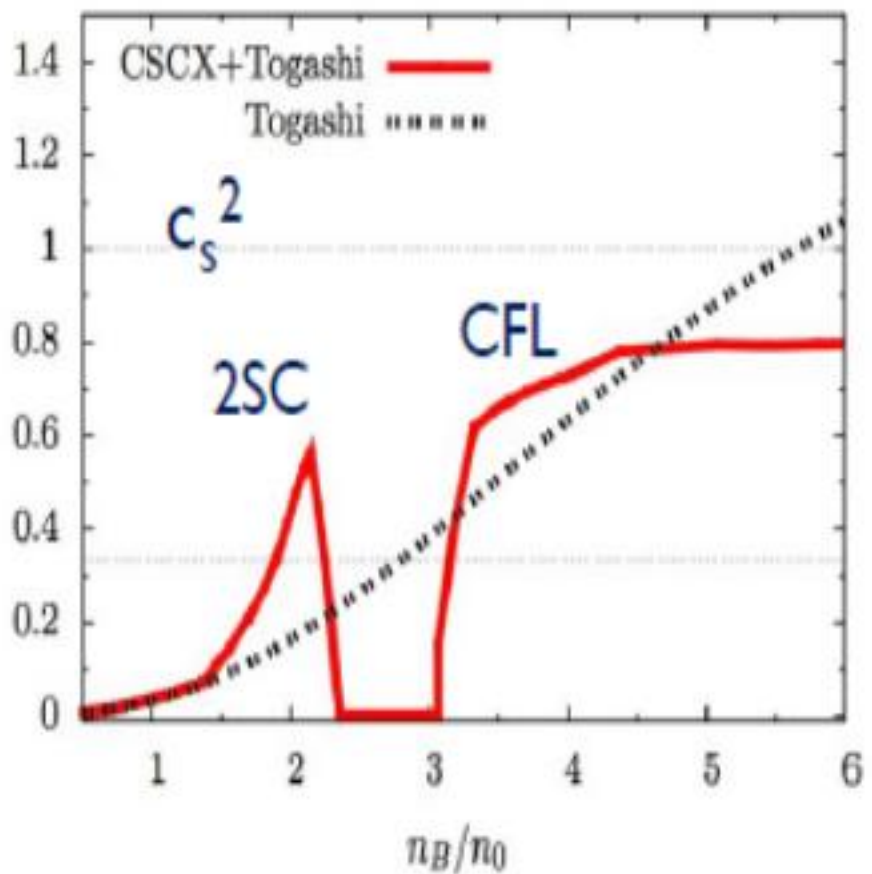
- 1) max. Freq. is determined by the speed of sound
- 2) Gluon condensate suppresses the energy density of GW and the max. freq.

Summary

Strongly interacting matter under extreme conditions has rich structures

- **QCD Phase diagram under rotation and Magnetic field**
- **EoS and Structure of NS**
- **GWs from 1OPT with gluon condensate**

Thank you very much for your attention!



The related vacuum energy at the PT is

$$\epsilon_* = \left(-\Delta F(T) + T \frac{d\Delta F(T)}{dT} \right) \Big|_{T=T_*}$$

One key parameter in phase transition gravitational wave

$$\alpha = \frac{\epsilon_*}{\rho_{\text{rad}}^*} = \frac{\epsilon_*}{\frac{\pi^2}{30} g_* T_*^4}$$

Hubble parameter at the temperature T_*

$$H_* = \sqrt{\frac{8\pi^3 g_*}{90}} \frac{T_*^2}{m_{pl}}$$

The contribution of the GW energy density from phase transition

$$h^2 \Omega(f) = h^2 \Omega_{en}(f) + h^2 \Omega_{sw}(f) + h^2 \Omega_{tu}(f)$$

$$\begin{aligned}
h^2 \Omega_{en}(f) &= 3.5 \times 10^{-5} \left(\frac{0.11 v_b^2}{0.42 + v_b^2} \right) \left(\frac{H_*}{\tau} \right)^2 \left(\frac{\kappa \alpha}{1+\alpha} \right)^2 \left(\frac{10}{g_*} \right)^{\frac{1}{3}} S_{en}(f) \\
h^2 \Omega_{sw}(f) &= 5.7 \times 10^{-6} \left(\frac{H_*}{\tau} \right) \left(\frac{\kappa_v \alpha}{1+\alpha} \right)^2 \left(\frac{10}{g_*} \right)^{\frac{1}{3}} v_b S_{sw}(f) \\
h^2 \Omega_{tu}(f) &= 7.2 \times 10^{-4} \left(\frac{H_*}{\tau} \right) \left(\frac{\kappa_{tu} \alpha}{1+\alpha} \right)^{\frac{3}{2}} \left(\frac{10}{g_*} \right)^{\frac{1}{3}} v_b S_{tu}(f)
\end{aligned}$$

The spectral shapes of GWs are characterized by the numerical fits as

$$S_{en}(f) = \frac{3.8 \left(\frac{f}{f_{en}} \right)^{2.8}}{1 + 2.8 \left(\frac{f}{f_{en}} \right)^{3.8}}$$

Peak frequency of each GW spectrum

$$f_{en} = 11.3 \times 10^{-9} [\text{ Hz}] \left(\frac{f_*}{\tau} \right) \left(\frac{\tau}{H_*} \right) \left(\frac{T_*}{100\text{MeV}} \right) \left(\frac{g_*}{10} \right)^{\frac{1}{6}}$$

$$S_{sw}(f) = \left(\frac{f}{f_{sw}} \right)^3 \left(\frac{7}{4 + 3 \left(\frac{f}{f_{sw}} \right)^2} \right)^{\frac{7}{2}}$$

$$f_{sw} = 1.3 \times 10^{-8} [\text{ Hz}] \left(\frac{1}{v_b} \right) \left(\frac{\tau}{H_*} \right) \left(\frac{T_*}{100\text{MeV}} \right) \left(\frac{g_*}{10} \right)^{\frac{1}{6}}$$

$$S_{tu}(f) = \frac{\left(\frac{f}{f_{tu}} \right)^3}{\left(1 + \frac{f}{f_{tu}} \right)^{\frac{11}{3}} \left(1 + \frac{8\pi f}{h_*} \right)}$$

$$f_{tu} = 1.8 \times 10^{-8} [\text{ Hz}] \left(\frac{1}{v_b} \right) \left(\frac{\tau}{H_*} \right) \left(\frac{T_*}{100\text{MeV}} \right) \left(\frac{g_*}{10} \right)^{\frac{1}{6}}$$

BH thermodynamics of hot dense hQCD

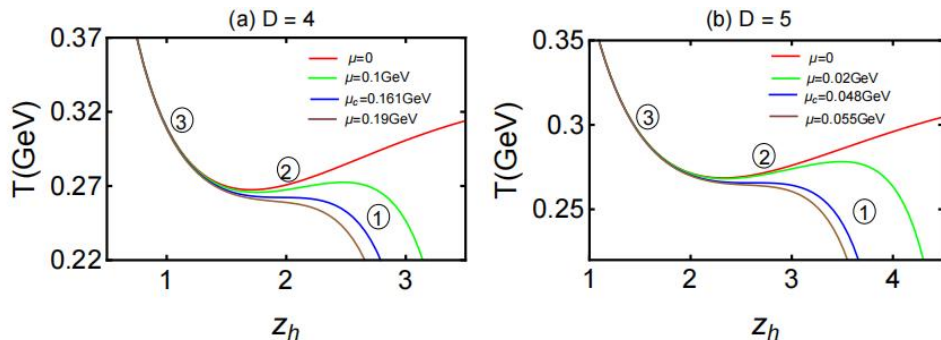


图16. D维下温度跟视界关系

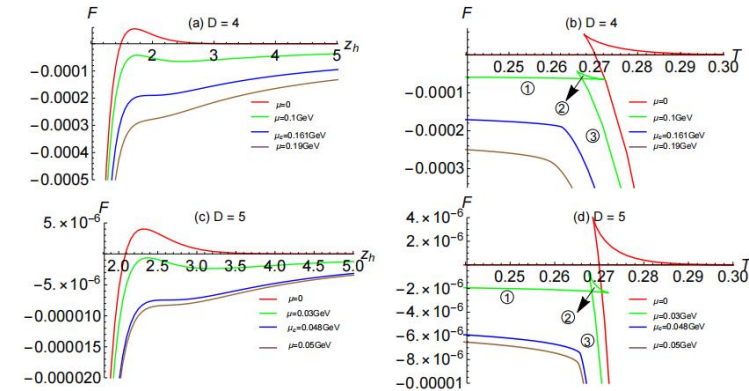


图17. D维下的自由能

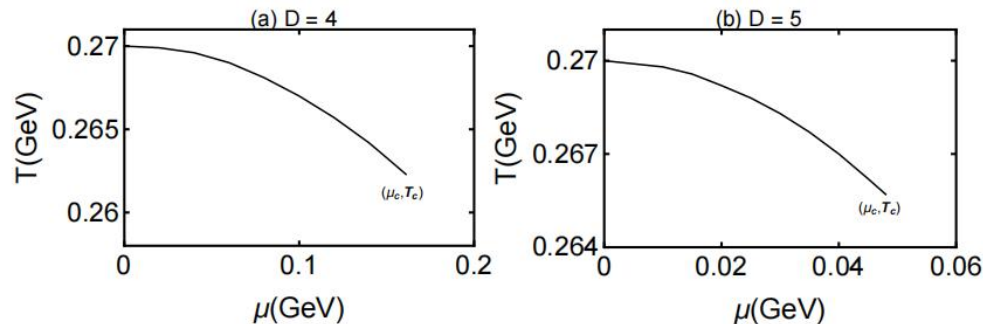


图18. D维下相图

- 1) 一阶相变附近温度、自由能非单调；平滑过渡附近单调；
- 2) 维度较低时，临界 μ_{CEP} 更大